An Optimal Excitation Method in Multi-Applicator Systems for Forming a Hot Zone Inside the Human Body

NAGAYOSHI MORITA, SENIOR MEMBER, IEEE, TAKESHI HAMASAKI, AND NOBUAKI KUMAGAI, FELLOW, IEEE

Abstract—**A method is proposed for determining the excitation amplitude and phase of each applicator in electromagnetic multi-applicator systems for forming a narrow high temperature zone inside the human body. The principal advantage of this method for determining the optimal amplitudes and phases is its simplicity and reasonableness. The general principle is explained by using the example of an elliptical body region, heated by several line current sources placed outside the body.**

Numerical examples are presented for the case where a human abdominal region composed of muscular and spinal layers surrounded by a cooling water layer is excited by several line sources at 40.68 MHz.

I. Introduction

FOR THE EFFECTIVE hyperthermia treatment, it is necessary to focus heat energy on a small region around the tumor to be treated. Developing a suitable apparatus for this purpose has become an interesting problem in biomedical engineering. When tumors are seated deep inside the human body, it is impossible, in practice, to concentrate heat energy just around the tumor region by a single applicator. Thus, the idea of using multiple applicators, or an electromagnetic multi-applicator system, is naturally reached [1]–[4]. There is, however, an inherent problem such that the electromagnetic energy cannot penetrate deep if the frequency is not sufficiently low, meanwhile if the frequency is low the focusing ability will be greatly reduced. This 'dilemma' would be very difficult to overcome if we desire to create extremely narrow heating spots for deep-seated tumors. Thus, an alternate solution to this problem would be to form a hot "zone" around the tumor region, particularly in anticipation of the fact that the tumor tends to absorb more heat energy than the normal tissue because of sluggish blood flow. Even then, remain the problems of what energy distribution patterns we should aim at and how we should determine the excitation amplitudes and phases, and the location of applicator elements. It is not a trivial problem to determine the optimum combination of these parameters, particularly when the number of applicators increases. Arcangeli *et al.* [5] have presented a direct optimization method for focusing 915-MHz electromagnetic power on deep-seated tissues in the chest region. Although this direct method is apparently reasonable and promising, the method leaves difficult problems such as the limitation in the depth of the focal position and the uncertainty as to the generality of the optimized solution.

This paper proposes a simple method of determining the optimal excitation amplitudes and phases of the applicator elements, for forming a hot zone around the tumor region. The main point of this method is to determine the amplitude and phase by means of the process of minimizing the norm of the difference between the resultant field distribution and the desirable field distribution for the chosen frequency [6]. The obtained energy distribution patterns may only be moderately focused but these are the best patterns we could attain.

II. Basic Principles

The human body is considered to be a lossy dielectric object electrically consisting of mainly two kinds of medium, that is, tissues of high water content (high loss) and low water content (relatively low loss). The magnitude of heat source causing the temperature rise is directly proportional to the electromagnetic power loss. Therefore, to study the problem in detail we must first solve the electromagnetic boundary value problem of dielectric objects with some sources placed near them. Since the fields, whose electric field is tangential to the boundary interface between two media of different dielectric constants can smoothly penetrate its boundary [7], the applicators' radiating fields with the electric field polarized in the axial direction seem to be suitable for deep heating the inside of an elliptical shaped region of the body such as the abdominal region. Taking these facts into consideration, we explain the principle of present method by assuming that axially directed line-current sources are placed around a cylinder of abdominal cross-sectional shape.

Let the current source i_i produce the electric field distribution $e_i(\rho)$ (ρ; position vector) in the abdominal cross section, and $E(\rho)$ be the total electric field distribution

Manuscript received June 22, 1985; revised October 12, 1985.

The authors are with the Department of Communication Engineering, Faculty of Engineering, Osaka University, Suita-shi, Osaka 565, Japan.

IEEE Log Number 8607840.

produced by all sources, that is,

$$E(\rho) = \sum_{i=1}^{M} a_i e_i(\rho) \tag{1}$$

where M is the number of sources and a_i is the constant coefficients. We determine the optimal values of a_i by minimizing the following number Ω, the square of the norm, given by

$$\Omega = \|\boldsymbol{E}_0 - \boldsymbol{E}\|^2 \tag{2}$$

where $\boldsymbol{E}_0$ and $\boldsymbol{E}$ are the vectors corresponding to the predetermined desirable electric-field distribution and the distribution obtained from the real sources, respectively. Both are assumed to be the elements of the p-dimensional vector space. The elements of this space are formed from the values of the electric-field distribution at the prespecified p test points in the cross-sectional area. We define the norm here by

$$\|\boldsymbol{E}_t\| = \left\{ \sum_{t=1}^{p} W_t |E_t(t)|^2 \right\}^{1/2} \tag{3}$$

where W_t is the proper weighting constant, and $E_t(t)$ is the value of the vector $\boldsymbol{E}_t$ at the point t. Solving numerically the linear equations obtained from $\partial\Omega/\partial\bar{a}_i = 0$ (where the bar "$-$" means the complex conjugate), we can obtain the optimal values of a_i $(i=1,2,\cdots,M)$. The a_i thus determined gives the optimal value directly for the excitation amplitude and phase of the ith current source, since the mapping from the space whose elements are i_i's to the space whose elements are e_i's is isomorphic. What kind of distribution should be chosen as $\boldsymbol{E}_0$ is the remaining essential problem. This $\boldsymbol{E}_0$ should be a realizable and desirable distribution. We propose to choose as $\boldsymbol{E}_0$ the set of values (at the p test points) obtained using the function $CJ_0(k\rho)$ where J_0 is the 0th-order Bessel function, C is a constant, k is the complex wavenumber of the muscle medium surrounding the tumor, and ρ is the radius measured from the center position of the tumor region. We should note that $J_0(k\rho)$ is simply the solution of the wave equation for the muscle medium. We could make the distribution narrower than the $J_0(k\rho)$ shape in one angular direction, but then the distribution in the other directions widens, necessarily.

Once the electric field e_i is calculated numerically for every i_i with its location given, we can easily and logically determine the optimal excitation amplitudes and phases of the sources. This idea is quite general and applicable to any kind of applicator that radiates the electric polarized fields in the axial direction.

III. Application to the Human Abdominal Region

As a model of analysis we choose an elliptical-shaped body region composed of muscle and spine layers, typical of the abdominal region. A cooling water layer surrounded on the outside with M line-current sources is present. This geometry is shown in Fig. 1, together with the dimensions (in centimeters) used for the numerical illustration.

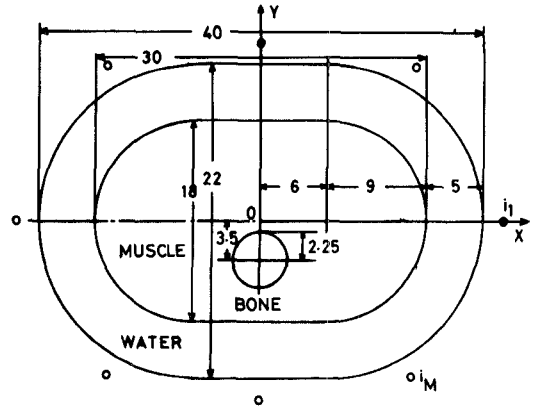

Fig. 1. A model for the human abdominal region (in centimeters).

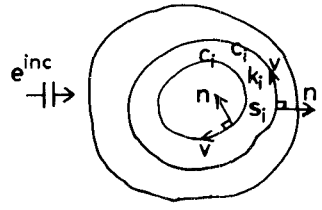

Fig. 2. General geometry pertaining to the integral equation formulation.

In the whole process of the present method, the analysis of electric-field distribution $e_i(\rho)$ in the body region produced by i_i needs the most lengthy numerical process. Once $e_i(\rho)$ corresponding to each i_i is obtained, the optimal values of a_i are easily determined, provided that the mutual interaction among sources can be neglected. The electric fields are obtained here mainly by means of the surface integral equation approach in which the unknowns are the tangential electric and magnetic fields on the boundary surfaces. The basic equations used are [8]

$$e^{inc} + \frac{j}{4}\int_{c_i}\left(\frac{\partial e}{\partial n'}\psi_f - e\frac{\partial \psi_f}{\partial n'}\right) dv' = \frac{1}{2}e, \qquad \rho \in c_i \tag{4}$$

$$= e, \qquad \rho \in s_i \tag{5}$$

where

$$\psi_f = H_0^{(2)}(k_i R), \qquad R = |\rho - \rho'| \tag{6}$$

with $H_0^{(2)}$ being the 0th order Hankel function of the second kind, and e^{inc} is the incident electric field excited by the sources, and is zero except in the outermost region where sources are placed. s_i and c_i are the ith homogeneous region and the boundary line of the region s_i, respectively (see Fig. 2). n and v are the coordinates along the outward normal and tangent directions at a point on c_i, respectively. k_i is the wave number in the region s_i. The prime stands for the integration coordinate. One point we must pay attention to in (4) is that the integral equation of this type does not necessarily give unique solutions, in other words, the nonphysical resonant solutions are present [9]. For the present problem, however, these nonphysical solutions can be ignored because the lowest resonant solution appears when the scatterer dimension is greater than 0.7λ (where λ is the wavelength of the outermost medium)

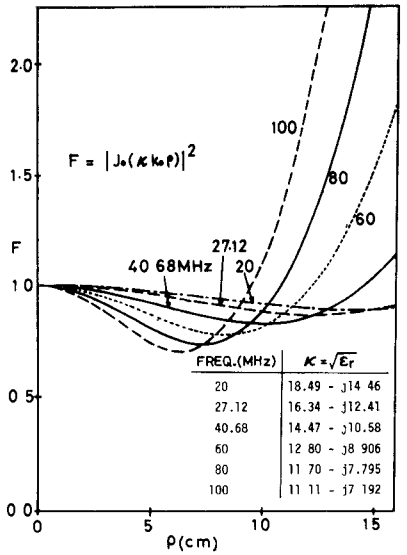

Fig. 3. Desirable power dissipation distribution in unbounded muscle region.

and λ is assumed here to be several meters while the body dimension is usually shorter than 1 m.

The electric field $e_t(\rho)$ could be calculated by other methods, e.g., the volume type integral equation [10], [11], the finite difference [12], and the finite element. These methods will be needed when the inhomogeneous properties of the body must be taken into account. In the present paper, however, the inhomogeneity of the body is not so important since the wavelength used here is relatively long (about 50 cm in muscle). In Section IV a numerical example will include some inhomogeneity in the muscle region. For this example, the volume-type integral equation using a polarization current model [10] is used additionally for evaluating this inhomogeneity.

IV. Numerical Illustration and Discussion

Fig. 3 depicts the values of the function F, viz.,

$$F = |E_0|^2, \quad E_0 = J_0(\kappa k_0 \rho) \tag{7}$$

for several frequencies where k_0 is the free-space wavenumber and κ is the complex refractive index in the muscle medium. The κ values used are inserted in the figure [13]. The function F corresponds to the power dissipation distribution (in the unbounded muscle region) with rotational symmetry with its center at $\rho = 0$; this is also the desirable heat source distribution that we aim at, since the power dissipation distribution is proportional to the heat source distribution. We see from Fig. 3 that the higher frequencies have the greater advantage of forming a narrower central hot zone but they make the larger ρ-region extremely hot. Cooling water will serve to lower the temperature in this region. Here, a question would arise why the function F is chosen such that the outer region is hotter than the central region. One answer to this question is that any other artificial functions might meet with the problem of realizability.

The present numerical examples employ the frequency of 40.68 MHz. All the sources are placed 2-cm apart from the

TABLE I
Dielectric Constants and Conductivities

Regions	ϵ_1	σ_1 (mmho/m)
Bone [13]	14.6 - j7.85	17.8
Muscle [13]	97.3 - j306	693
Bowel	80.0 - j31.0	70.2
Water [14]	78.1 - j0.0	0.0

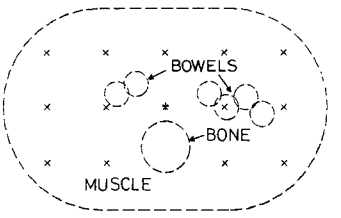

Fig. 4. Location of test points and bowel regions.

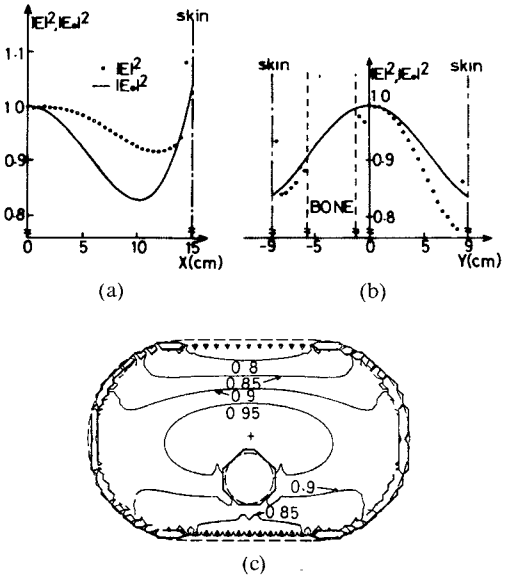

Fig. 5. Power dissipation distribution for the sources excited in equal amplitudes and phases; $M = 8$. (a) On the x-axis. (b) On the y-axis (c) Contour lines.

outer boundary of the water layer at equal angular intervals with one source on the positive x-axis (Fig. 1). The values of the dielectric constant ϵ_t and conductivity σ_t used in each region are shown in Table I [13], [14]. The test points used for forming the vector $\boldsymbol{E}$ are placed only within the muscle region and spaced equally in the x and y directions, respectively. All W_t are chosen as 1. The locations of p's are shown by $\times$ marks in Fig. 4 and $p = 14$ is fixed throughout the paper. It was checked that the difference of the p value does not have a large influence on the results and that the larger p is not necessarily preferable.

Fig. 5 plots the values of $|E|^2$, which are proportional to the power dissipation distribution, for the case of eight-line sources, that is, $M = 8$. All the sources are excited with equal amplitudes and phases. The dotted lines in Fig. 5(a) and (b) represent the values on the two principal planes, along x- and y-axes, respectively. The solid lines on Fig. 5(a) and (b) represent the desirable distribution $|E_0|^2$ obtained from (7). Both $|E|^2$ and $|E_0|^2$ in Fig. 5(a) and (b)

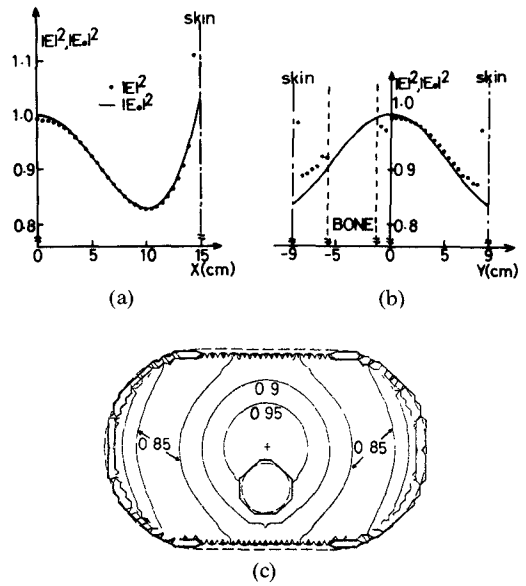

Fig. 6. Power dissipation distribution for the sources optimally excited; focus is on the origin and $M = 8$. (a) On the x-axis. (b) On the y-axis. (c) Contour lines.

are normalized to the value $|E_0|^2$ at the origin ($x = 0$, $y = 0$). The contour lines of equal power dissipation are depicted in Fig. 5(c). The complicated winding curves appearing near the outer boundary of the muscle region come from the deterioration of the accuracy in calculating electric fields, and should be discarded. This deterioration in accuracy also causes abnormally large values for a few points near the outer boundaries in Fig. 5(a) and (b). The inaccuracy comes from the crudeness of the numerical integration process used for obtaining the values in the interior region after solving integral equations and it occurs only when the observation points are very close to the boundary peripheral lines. We will comment later on the accuracy of the present method. We may disregard these inaccurate values near the outer boundary because it is expected that in a practical situation the body will be cooled from the outside to avoid excess heating near the superficial region of the body. This is the reason that Fig. 1 includes the water layer. The power loss distribution in the spinal region is not shown here because its quantity becomes very small compared to that in the muscular region (the conductivity in the bone is generally considerably smaller than that in the muscle medium). Fig. 4 indicates that the uniform excitation due to identical sources produces a distribution pattern elongated in the lateral direction.

Fig. 6 shows the corresponding results for the case where the excitation amplitudes and phases of eight-line sources ($M = 8$) are optimized using the present method. The origin ($x = 0$, $y = 0$) is the focus or the target position, that is, the point where $\rho = 0$. The values $|E|^2$ and $|E_0|^2$ are both normalized to the value $|E_0|^2$ at the target position in Fig. 6(a) and (b), and also in all other similar figures shown afterwards. Fig. 6 indicates that, different from the case of the uniform excitation, the resultant distribution agrees closely with the desirable one except in the regions near the

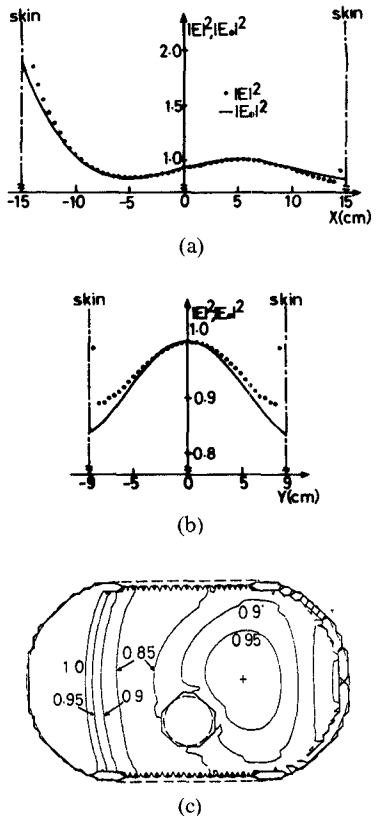

Fig. 7. Power dissipation distribution for the sources optimally excited; focus is on the point (5.0 cm, 0.0) and $M = 6$. (a) On the x-axis. (b) On the $x = 5.0$-cm line. (c) Contour lines.

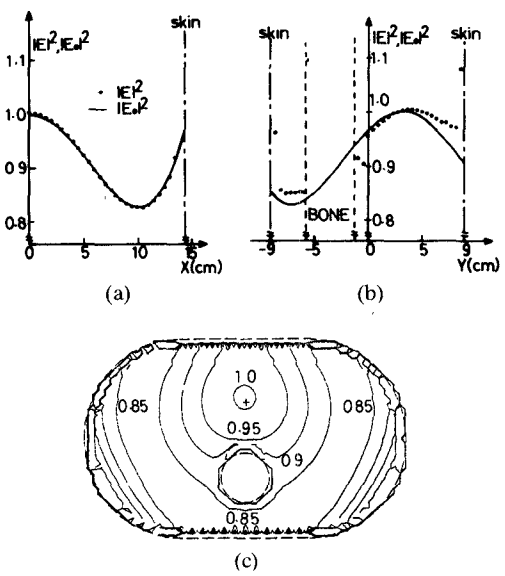

Fig. 8. Power dissipation distribution for the sources optimally excited; focus is on the point (0.0, 3.15 cm) and $M = 8$. (a) On the $y = 3.15$-cm line. (b) On the y-axis. (c) Contour lines.

spinal and the outer boundaries. Although the results are not shown here, the cases of $M = 6$ and $M = 4$ were also calculated and it was found that the curves and contours were almost the same as those in Fig. 6(a) and (b).

Fig. 7 is an example when the target position is not at the origin but at ($x = 5.0$ cm, $y = 0.0$) with $M = 6$. Similar curves and contours are obtained for $M = 8$ and $M = 4$

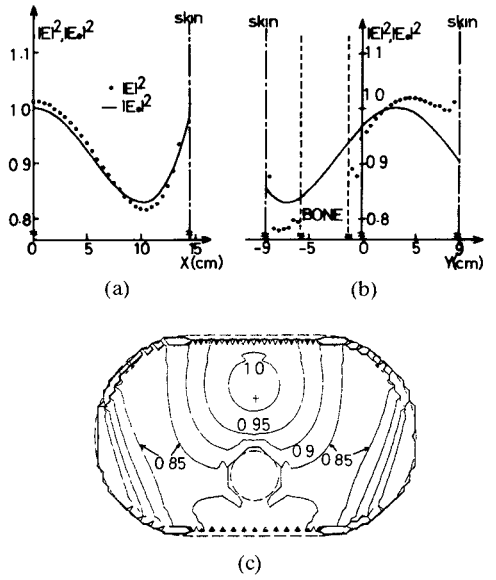

Fig. 9. Power dissipation distribution for the sources optimally excited; focus is on the point (0.0, 3.15 cm) and $M = 6$. (a) On the $y = 3.15$-cm line. (b) On the y-axis. (c) Contour lines.

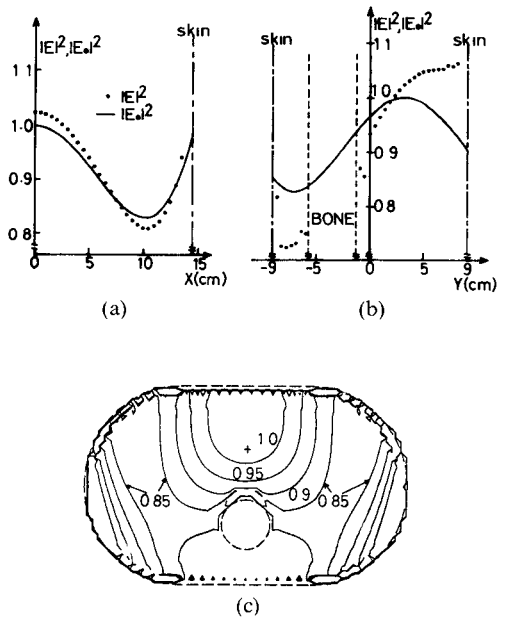

Fig. 10. Power dissipation distribution for the sources optimally excited; focus is on the point (0.0, 3.15 cm) and $M = 4$. (a) On the $y = 3.15$-cm line. (b) On the y-axis. (c) Contour lines.

also. Again the resultant distribution agrees closely to the desirable one. However, when the target position is moved along the y-axis direction, the realization of the desirable pattern with only four sources seems to become slightly more difficult. This can be seen by comparing Figs. 8, 9, and 10, the examples of the target position being placed at ($x = 0.0$, $y = 3.15$ cm). Figs. 8, 9, and 10 are for $M = 8$, 6, and 4, respectively.

Next, some simple examination will be made for the case where the muscle region is not homogeneous. In this example, the cross sectional shape has two bowel regions as

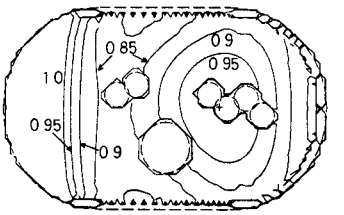

Fig. 11. Optimized power loss contour lines for the cross-sectional shape with bowel regions; focus is on the point (5.0 cm, 0.0) and $M = 6$.

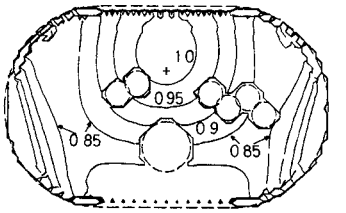

Fig. 12. Optimized power loss contour lines for the cross-sectional shape with bowel regions; focus is on the point (0.0, 3.15 cm) and $M = 6$.

shown in Fig. 4 by the set of six dashed circles. This shape was determined by referring to actual computed tomography images. In the calculation of $e(\rho)$ for this shape, the volume-type integral equations as applied to the bowel regions are used additionally. The electric field in the bowel regions is assumed constant over each circle [10] and hence the number of unknowns increases by six. The area of each circle is chosen to be 4 cm^2, the radius being about 1.13 cm. The dielectric constant in the bowels is assumed to be $80.0 - j31.0$ which is obtained from the weighted average ($0.9 \times$ dielectric constant of water plus $0.1 \times$ that of muscle). This value is typical since the dielectric constant for bowels varies depending upon the contents packed in the bowels. One example of the optimized power loss distribution for this cross-sectional shape is shown in Fig. 11, in which the contour lines are drawn, where the target is at ($x = 5.0$ cm, $y = 0.0$), and $M = 6$. The obtained result is found to be almost unchanged from that of Fig. 7. Although not shown here, the results for both $M = 4$ and $M = 8$ do not differ much. From Fig. 4 one test point is inside the bowel region. This test point, however, has almost no effect on the result. The power loss distribution remains unchanged even if this point in the bowels is removed from the set of test points. Fig. 12 shows the power loss contour lines with the target at ($x = 0.0$, $y = 3.15$ cm) and $M = 6$. The contour line patterns of Figs. 11 and 12 look similar to the corresponding patterns for the cases without bowels in Figs. 7 and 9, respectively. Thus we can conclude that the present method will not be seriously affected by the presence of inhomogeneities such as the bowels. This advantage is due to the facts that in our examples the electric field is polarized in a parallel direction to the boundaries of the bowel regions and least-mean-square matching is employed.

Since the power deposition is evaluated in this paper only in the muscle medium with a uniform physical con-

TABLE II
OPTIMIZED AMPLITUDES AND PHASES

Figure \ Applicator No.		1	2	3	4	5	6	7	8
Fig.6	Amp.	1.0	0.8123	0.3361	0.8124	0.9999	0.9441	0.6556	0.9441
	Phase	0.0	-22.8	156.3	-22.8	0.0	-25.7	147.6	-25.7
Fig.7	Amp.	1.0	0.1115	0.6168	2.5278	0.5520	0.1011		
	Phase	0.0	-70.2	0.9	38.8	2.5	-118.7		
Fig.8	Amp.	1.0	0.5881	0.5910	0.5880	1.000	1.1972	0.4228	1.1972
	Phase	0.0	-36.7	143.6	-36.7	0.0	-7.6	169.7	-7.6
Fig.9	Amp.	1.0	0.0320	0.0313	1.000	0.3414	0.3415		
	Phase	0.0	-144.6	-144.5	0.0	5.0	5.0		
Fig.10	Amp.	1.0	0.1431	1.000	0.4584				
	Phase	0.0	-167.3	0.0	12.1				
Fig.11	Amp.	1.0	0.1288	0.3798	2.3181	0.3517	0.1626		
	Phase	0.0	-159.5	-1.6	35.7	0.2	-166.3		
Fig.12	Amp.	1.0	0.1203	0.0948	1.0184	0.2703	0.2439		
	Phase	0.0	173.6	173.9	-0.5	17.1	21.4		

stant (except in Figs. 11 and 12), its relative value can be evaluated by the square of absolute value of the electric field. However, if the power deposition is needed in various kinds of media with different physical constants, the square of the absolute value of the electric field must be multiplied by the conductivity value for the corresponding medium. The dissipated power value thus obtained varies drastically from media to media because of a great difference in their conductivity values. Hence, if the models are more inhomogeneous, the dissipated power value will considerably change from place to place as in [5], [15], and [16]. Even then, the square of absolute value of the electric field must remain comparatively unchanged from place to place, provided that the model is two-dimensional, the electric field is polarized in the axial direction, and the frequency is relatively low. This is one reason why we chose here the almost homogeneous models and used mostly the surface integral equation formulation.

The excitation amplitudes and phases actually obtained following the present optimization method are tabulated in Table II, in which the relative values to those of the applicator number 1 are given. It would be impossible to arrive at these complicated values experimentally only or empirically. It is interesting to notice that the amplitude and phase values given for the applicators on the y-axis for $M = 8$ (Fig. 8) are considerably different from those for $M = 4$ (Fig. 10), and that the values for the cases with bowels (Figs. 11 and 12) are, as expected, somewhat different from those for the corresponding cases without bowels (Figs. 7 and 9, respectively). For the examples of Figs. 6, 8, 9, and 10, the values for the applicators located symmetrically with respect to the y-axis must be equal if the accuracy is sufficient. Table II shows that this symmetrical property is satisfied up to the third or the fourth significant figure.

Accuracy of the calculation can be checked by various means. One of them is to check the degree of satisfaction of the energy conservation that holds among the dissipated power, scattered power, and the net power extracted from all sources. The relative error with respect to this energy conservation was checked for all numerical examples performed. The relative error in the worst case of Figs. 4–10 was 3.9%, and those for Figs. 11 and 12 were 3.0% and 4.2%, respectively.

Once the power loss distribution is obtained, the next problem will be to evaluate the time evolution of temperature distribution with this power loss distribution as the heat source distribution. To investigate the latter problem theoretically, we have to solve the heat conduction equation. We would be able to guess intuitively the time evolution of temperature distribution for the present problem if we refer to [17], in which by using the cross-sectional shape similar to that used here the cooling effect of the water layer is mainly investigated.

V. CONCLUSION

A simple method has been proposed for obtaining the optimal excitation amplitudes and phases of multi-sources placed around the elliptical body to heat deep inside the body. The method has been demonstrated through numerical illustrations to be very effective in forming a hot zone around the tumor region. It was found that relatively small number of sources suffice this purpose. Studies for the cases of distributed sources more akin to the practical applicators as well as a parametric study remains to be done. It will also be very interesting to examine the results of the present method as applied to the more inhomogeneous models corresponding to computer tomography images.

REFERENCES

[1] M. Melek and A. P. Anderson, "Theoretical studies of localized tumor heating using focused microwave arrays," *Proc. Inst. Elec. Eng.*, vol. 127, Pt.F, pp. 319–321, Aug. 1980.

[2] R. Knoechel, "Capabilities of multiapplicator systems for focused hyperthermia," *IEEE Trans. Microwave Theory Tech.*, vol. MTT-31, pp. 70–73, Jan. 1983.

[3] P. F. Turner, "Regional hyperthermia with an annular phased array," *IEEE Trans. Biomed. Eng.*, vol. BME-31, pp. 106–114, Jan. 1984.

[4] F. A. Gibbs, M. D. Sapozink, K. S. Gates, and J. R. Stewart, "Regional hyperthermia with an annular phased array in the experimental treatment of cancer: Report of work in progress with a technical emphasis," *IEEE Trans. Biomed. Eng.*, vol. BME-31, pp. 115–119, Jan. 1984.

[5] G. Arcangeli, P. P. Lombardini, G. A. Lovisolo, G. Marsiglia, and M. Piattelli, "Focusing of 915 MHz electromagnetic power on deep human tissues: A mathematical model study," *IEEE Trans. Biomed. Eng.*, vol. BME-31, pp. 47–52, Jan. 1984.

[6] N. Morita and T. Hamasaki, "A method of forming a hot zone inside the human body in electromagnetic hyperthermia therapy," in *IEEE EMC-S Int. Electromagnetic Compatibility Symp. Dig.*, Oct. 1984, pp. 354–359.

[7] N. Morita and J. Bach Andersen, "Near-field absorption in a circular cylinder from electric and magnetic line sources," *Bioelectromag.*, vol. 3, pp. 253–274, 1982.

[8] T. K. Wu, and L. L. Tsai, "Scattering by arbitrarily cross-sectioned layered lossy dielectric cylinders," *IEEE Trans. Antennas Propagat.*, vol. AP-25, pp. 518–524, July 1977.

[9] N. Morita, "Resonant solutions involved in the integral equation approach to scattering from conducting and dielectric cylinders,"

IEEE Trans. Antennas Propagat., vol. AP-27, pp. 869–871, Nov. 1979.
[10] J. H. Richmond, "Scattering by a dielectric cylinder of arbitrary cross section shape," *IEEE Trans. Antennas Propagat.*, vol. AP-13, pp. 334–341, May 1965.
[11] D. E. Livesay and K. M. Chen, "Electromagnetic fields induced inside arbitrarily shaped biological bodies," *IEEE Trans. Microwave Theory Tech.*, vol. MTT-22, pp. 1273–1280, Dec. 1974.
[12] O. P. Gandhi, J. F. Deford, and H. Kanai, "Independence method for calculation of power deposition patterns in magnetically induced hyperthermia," *IEEE Trans. Biomed. Eng.*, vol. BME-31, pp. 644–651, Oct. 1984.
[13] J. C. Lin, A. W. Guy, and C. C. Johnson, "Power desposition in a spherical model of man exposed to 1–20-MHz electromagnetic fields," *IEEE Trans. Microwave Theory Tech.*, vol. MTT-21, pp. 791–796, Dec. 1973.
[14] R. F. Harrington, *Time-Harmonic Electromagnetic Fields*. New York: McGraw-Hill, 1961, Appendix B.
[15] M. F. Iskander, P. F. Turner, J. B. Dubow, and J. Kao, "Two-dimensional technique to calculate the EM power deposition pattern in the human body," *J. Microwave Power*, vol. 17, pp. 175–185, 1982.
[16] P. M. van den Berg, A. T. De Hoop, A. Segal, and N. Praagman, "A computational model of the electromagnetic heating of biological tissue with application to hyperthermic cancer therapy," *IEEE Trans. Biomed. Eng.*, vol. BME-30, pp. 797–805, Dec. 1983.
[17] N. Morita, "Integral equation formulation for heat conduction in closed regions with arbitrarily shaped boundary surfaces," *J. Appl. Phys.*, vol. 56, pp. 1987–1991, Oct. 1, 1984.

✠

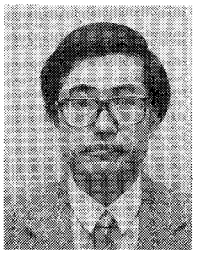

Nagayoshi Morita (M'67–SM'84) was born in Japan, on March 28, 1942. He received the B.S., M.S., and Ph.D. degrees in communication engineering from Osaka University, Suita-shi, Japan, in 1964, 1966, and 1977, respectively.

Since 1966, he has been with the Department of Communication Engineering, Osaka University, Suita-shi, Japan, where he has been working on millimeter and optical waveguides, analytic and numerical techniques for electromagnetic wave problems, hyperthermia, etc. From September 1979 to June 1980, he stayed in Denmark on a research scholarship, the first six months at Aalborg University Center and the last four months at the Technical University of Denmark.

Dr. Morita is a member of the Institute of Electronics and Communication Engineers of Japan, the Japan Society of Medical Electronics and Biological Engineering, and the Japanese Society of Hyperthermic Oncology.

Takeshi Hamasaki was born in Osaka, Japan, on April 6, 1960. He received the B.S. and M.S. degrees in communication engineering from Osaka University, Suita-shi, Japan, in 1984 and 1986, respectively.

Since 1986, he has been employed by Matsushita Electric Industrial Company Limited, Kadoma-shi, Osaka, Japan.

Mr. Hamasaki is an associate member of the Institute of Electronics and Communication Engineers of Japan.

✠

Nobuaki Kumagai (M'59–SM'71–F'81) was born in Ryojun, Japan, on May 19, 1929. He received the B. Eng. and D. Eng. degrees from Osaka University, Osaka, Japan, in 1953 and 1959, respectively.

From 1956 to 1960, he was a Research Associate in the Department of Communication Engineering at Osaka University. From 1958 through 1960, he was a Visiting Senior Research Fellow at the Electronics Research Laboratory of the University of California, Berkeley, while on leave of absence from Osaka University. From 1960 to 1970, he was an Associate Professor of Communication Engineering at Osaka University, and became Professor in 1971. From 1980 to 1982, he served as Dean of Students of Osaka University. From April of 1985, he has been Dean of Engineering of Osaka University, and has been a President of Osaka University since August of 1985.

His fields of interest are electromagnetic theory and its applications to the microwaves, millimeter-waves, and acoustic-waves engineering, optical fibers and related techniques, and lasers and their applications. He has published more than one hundred technical papers on these topics in established journals. He is the author or coauthor of several books, including *Microwave Circuits* and *Introduction to Relativistic Electromagnetic Field Theory*. From 1979 to 1981, he was Chairman of the technical group on Microwave Theory and Techniques of the Institute of Electronics and Communication Engineers of Japan. He is a member of the Telecommunications Technology Council of the Ministry of Post and Telecommunications and is a consultant for the Nippon Telegraph and Telephone Corporation (NTT).

Dr. Kumagai is Vice-President of the Institute of Electronics and Communication Engineers of Japan, member of the Institute of Electrical Engineers of Japan, and of the Laser Society of Japan. He has received the Achievement Award from the Institute of Electronics and Communication Engineers of Japan and the Special Award from the Laser Society of Japan. He was also awarded an IEEE Fellowship for contributions to the study of wave propagation in electromagnetics, optics, and acoustics.